



FR0301834
7NIS-FR-1909

CRYSTALLOGRAPHIC FATIGUE CRACK GROWTH IN A POLYCRYSTAL: SIMULATIONS BASED ON FEM AND DISCRETE DISLOCATION DYNAMICS

G. Bertolino^{1,2}, V. Doquet¹, M. Sauzay²

¹Laboratoire de Mécanique des Solides, Ecole Polytechnique, 91128 Palaiseau cedex, France

²CEA, DEN-DMN-SRMA, 91191 Gif-sur-Yvette cedex, France

bertolin@lms.polytechnique.fr

ABSTRACT

An attempt to model the variability of short cracks development in high-cycle fatigue is made by coupling finite element calculations of the stresses ahead of a microcrack in a polycrystal with simulations of crack growth along slip planes based on discrete dislocations dynamics. The model predicts a large scatter in growth rates related to the roughness of the crack path. It also describes the influence of the mean grain size and the fact that overloads may suppress the endurance limit by allowing arrested cracks to cross the grain boundaries.

INTRODUCTION

The behaviour of microstructurally small cracks is influenced by local crystallographic orientations resulting in a large scatter in fatigue lives specially in high-cycle fatigue.

Due to the elastic anisotropy of the grains the stress distribution in a polycrystal can be very heterogeneous. Moreover, the local texture influences both the ease of crack transfer beyond a grain boundary (GB) and the crack path orientation. The effective crack driving force varies substantially with the local microstructure.

The aim of the present work is to simulate the behaviour of short fatigue cracks by coupling finite element (FE) calculations with discrete dislocations dynamics (DDD)[1]. The stresses ahead of a microcrack in a polycrystal obtained by FE are used as input for the simulations of crack growth along slip planes by DDD. Simulations are performed for various random sets of crystal orientations and the scatter in predicted crack growth kinetics is analysed in relationship with local textures.

Low amplitude reversed torsion tests are performed on a 316L stainless steel and microcracks development monitored to provide data for the model.

EXPERIMENTAL OBSERVATIONS

The first reversed torsion test performed at ± 120 MPa on a specimen of 316L steel (mean grain size $50\mu\text{m}$) was periodically interrupted for observations of the microcracks. The specimen was not broken at 10^6 cycles. However, one grain size-long crystallographic microcracks initiated close to the maximum shear planes (longitudinal and transverse) and blocked by a GB were already present at 70000 cycles (less than 7% of the fatigue life). Fretting debris came out from the microcracks flanks. Arrest periods of at least 20000 cycles due to the GBs were measured. Sometimes, cracks became arrested soon after crossing a GB. This case was often associated with a large deflection of the crack plane. For this stress level, the transition to Stage II propagation occurred most often when the cracks were three grains

size-long. This transition did not always coincide with the transfer in a new grain but also occurred during transgranular propagation due to the activation of a secondary slip plane, 45° to the main crack direction. Early Stage II was still crystallographic, with a zig-zag crack path along two slip planes activated sequentially. Fatigue tests at different stress levels are in progress.

PRINCIPLE OF THE SIMULATIONS

The simulation process is divided into two main parts, the evaluation of the stress field near the crack tip by FE and the simulation of the crack growth by DDD.

The computation of the stress field is performed in elasticity, since high-cycle fatigue is considered, by using CAST3M FE code. The mesh consists of a circular multicrystal (~ 30 grains), containing a crack, embedded in a homogeneous medium (fig 1). The homogeneous medium constitutes a square plate on which borders global loading is applied. The mesh is refined in the grains containing the crack tip where the smallest elements are $0.05\mu\text{m}$ wide, so as to capture the associated stress concentration and gradient. The elastic constants for austenite grains are taken as: $C_{11}=197.5\text{GPa}$, $C_{12}=122\text{GPa}$ and $C_{44}=125\text{GPa}$ cubic symmetry, for the homogeneous medium they are $E=210\text{GPa}$ and $\nu=0.3$.

The K_I and K_{II} (stress intensity factor: SIF) are determined as the limit of $\sigma_{xx}\sqrt{(2\pi x)}$ and $\sigma_{xy}\sqrt{(2\pi x)}$, respectively, as x goes to zero (where x denotes the abscissa in a coordinate system centered at the crack tip with its first axis tangent to the local crack direction).

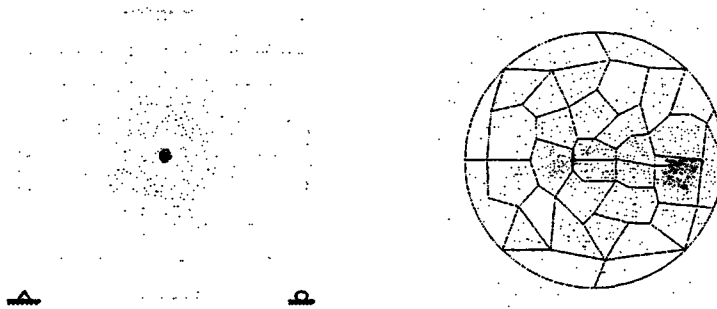


Figure 1: Mesh of the circular multicrystal embedded in a homogeneous medium

Since Stage I crystallographic propagation in FCC metals due to mixed mode I + II loading is modelled, the crack follows $\{111\}$ planes and its front is supposed to be normal to a $\langle -1\ 1\ 0 \rangle$ direction, so that the dislocations emitted at its tips have a pure edge character.

The SIFs are computed under maximum and minimum global stresses, since cyclic loading is considered, as well as the distribution of σ_{xy} in the crack plane, between the crack tip and the closest GB. These results are used as input for simulations of crack tip plasticity based on DDD. Even under fully reversed global loading, the loading path undergone by the crack is not symmetrical but is constituted with one segment in mixed mode I + II and one segment in pure shear. The mode I component is considered to assist crystallographic crack propagation when it is present but not to drive it.

The expression of the stress field generated by an infinite dislocation in an anisotropic elastic medium can be found after the resolution of a sextic equation whose coefficients depend on the elastic constants, the slip plane and the slip direction [2]. For an infinite edge dislocation

lying along the (1 -1 2) direction with a Burgers vector $b = a/2 (1 1 0)$ in a FCC crystal, the in plane shear component is of the form: $\mathbf{Ab}/2\pi x$, where A is a constant which depends on the roots of the sextic equation and in the present case, $A = 107\text{GPa}$.

The critical mode II stress intensity factor for the emission of a coplanar edge dislocation from the crack tip is calculated as a function of the mode mixity parameter Ψ :

$$K_{II}^{nucl} = \sqrt{2A[\gamma_{us}^r - \alpha(\gamma_{us}^u - \gamma_{us}^r)(\frac{\pi}{2} - \psi)]} \quad \text{where} \quad \psi = \text{Arctan}(\frac{K_{II}}{K_I}) \quad (1)$$

where α , γ_{us}^u and γ_{us}^r are materials parameters. Since $\gamma_{us}^u > \gamma_{us}^r$, eqn (1) predicts a lower threshold stress intensity factor for dislocation nucleation when Ψ decreases, that is, when an opening stress is present (for more details, see [3]).

The shear stress on the i^{th} dislocation at abscissa x_i in the plastic zone is evaluated as:

$$\tau_i = \sigma_{xy}(x_i) - \frac{Ab_i}{4\pi x_i} - \sum_{j \neq i} \frac{Ab_j}{2\pi} \sqrt{\frac{x_j}{x_i}} \frac{1}{x_j - x_i} \quad (2)$$

in which the three terms represent respectively the shear stress distribution ahead of the crack computed by FE, the image stress (the crack flanks are free surfaces) and the stress field of other dislocations. Strictly, this equation (as well as eqn (3)) is valid for a semi infinite crack [4]. The semi-infinite crack approximation is reasonable because in the present case, the free path of dislocations is limited by GBs the difference in predicted crack growth rates considering length or infinite finite has been found negligible.

The velocity of each dislocation is calculated as a power function of $\tau_i - \tau_f$ (τ_f is the lattice resistance to dislocation glide), see [1]. The new position of each dislocation is then deduced, and annihilation criteria checked: if a dislocation comes close enough to the crack tip or to a dislocation of opposite sign, it is removed from the simulation.

The dislocation emission criterion is checked to decide whether a negative or positive dislocation can be emitted:

$$K_{II}^{tip} \leq -K_{II}^{nucl} \quad \text{or} \quad K_{II}^{tip} \geq K_{II}^{nucl} \quad \text{where} \quad K_{II}^{tip} = K_{II} - \sum_{i=1}^n \frac{Ab_i}{\sqrt{2\pi x_i}} \quad (3)$$

This sequence is repeated until the second cycle is completed. Then, the crack growth rate per cycle is computed. The crack is considered to grow by one Burgers vector each time a pair of positive-negative dislocation has been emitted or when a dislocation returns to the crack tip since both events correspond to some cyclic plastic flow at the crack tip and should thus contribute to its growth.

Grain boundaries are considered as impenetrable obstacles for the dislocations emitted by the crack. This implies crack deceleration and arrest, unless a source is activated in the next grain, which, after an incubation period could initiate a crack that would link with the arrested one, thus allowing further propagation.

The stress concentration due to the pile up in the next grain is estimated as follows. Head [5] has shown that a dislocation of Burgers vector b in a medium of shear modulus μ_1 close and parallel to an interface with a different elastic medium, of modulus μ_2 , generates in this

medium the same stress field as a dislocation of Burgers vector $2\mu_1b/(\mu_1+\mu_2)$. The in-plane shear moduli of the grain containing the crack tip and that of his neighbour are thus computed in the coordinate system tangent to the crack tip. The stress field in the next grain is approximated with Head's formula and added to the elastic stress field computed by FE. The resolved shear stresses on the potential slip systems of the next grain which do not imply a twist of the crack plane are computed at a distance of $1\mu\text{m}$ from the GB. There are two reasons for this condition on the potential slip systems: first, the experimental work of Zhai et al [6] has shown that the path most likely to be followed by the crack is generally the one which minimises its twist deflection and second, the 2D nature of the model would not allow the description of 3D tortuosity of the crack path.

If one of the computed resolved shear stresses τ_{res} exceeds a critical value, τ_s , a source is considered to be activated and the number of cycles, N_{inc} , for crack initiation due to the activity of this source followed by linking with the arrested crack is estimated to be elapsed when,

$$\int_1^{N_{inc}} C(\tau_{res}(N)-\tau_s)^n dN=1 \quad (4)$$

where C and n are constants to be determined from experimental data on short cracks kinetics. Eqn (4) was inspired from the incubation model of Morris et al [7]. Ludwig et al [8] also report arrested microcracks in spite of a well visible plastic zone in the next grain. This means that the transfer of a crack tip beyond the boundary does not coincide with the activation of a slip system but requires a maturation time. When condition (4) is verified, a new mesh with a $1\mu\text{m}$ long branch crack in the next grain is generated and the whole process starts again.

The numerical values of the materials parameters used for the simulations are: $\gamma_{,US}^U=1.64\text{J.m}^{-2}$, $\gamma_{,US}^r=1.41\text{J.m}^{-2}$, $\alpha=1$, $\tau_f=58\text{ Mpa}$, $\tau_s=96\text{ MPa}$, $C=510^{-10}\text{MPa}^{1/n}$ and $n=2$. With these values, the dislocation emission threshold in pure shear is $0.55\text{MPa}\sqrt{\text{m}}$. Unless specified, the applied shear stress is $\pm 130\text{MPa}$ and the mean grain size $50\mu\text{m}$. The table in figure 2 defines the simulated crack paths.

RESULTS AND DISCUSION

The evolution of the maximum computed SIFs with microcracks length for crack paths n°1, 2 and 4 are plotted on figure 2. The evolution of K_{II} obtained using a uniform stress approximation ($K_{II}=\tau_{app}\sqrt{\pi a}$) appears to systematically overestimates K_{II} , because the most favourable grain orientation for crack initiation corresponds to a shear modulus which is only 83% of the average modulus on the one side, and the above-mentioned approximation is for a straight crack, whereas roughness shields the crack tip singularity, on the other side. Furthermore, K_{II} is highly variable from one microcrack to the other, depending on their paths. It does not systematically increase with the crack length but it may exhibit a sudden drop due to tilting at a GB. The mode mixity also shows abrupt variations and it may be surprisingly high for cracks which are not very far away from the nominally pure shear plane.

The computed arrest time at the first G.B. increases with the tilt angle of the crack plane in the next grain as: (28700, 4300, 9200, 33800, ∞) for tilt angles of (10, 20, 27, 35, 45°) respectively. Since in the orientation most favourable to initiation the microcrack is loaded in pure shear, the activation of a slip system at 45° -a principal plane- is impossible and in that case, the crack gets arrested. Note that it might be different in presence of a mode I component.

Figure 3 compares the evolution of the projected lengths for the different crack paths. For a given path, the incubation period due to GBs is smaller and smaller as the crack grows.

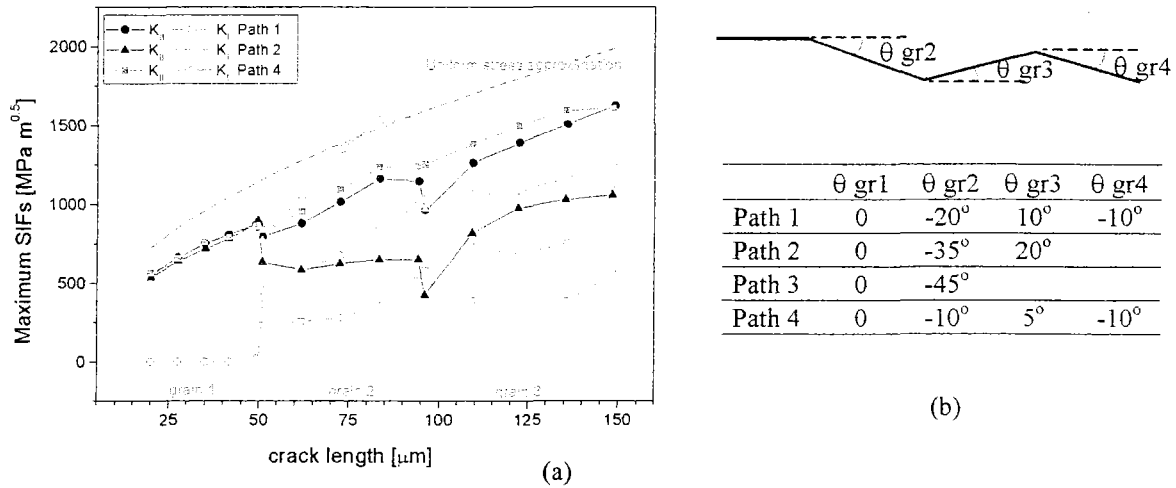


Figure 2. a- Evolution of the maximum computed SIFs with projected microcracks length for crack paths n°1, 2 and 4; b- crack path definition.

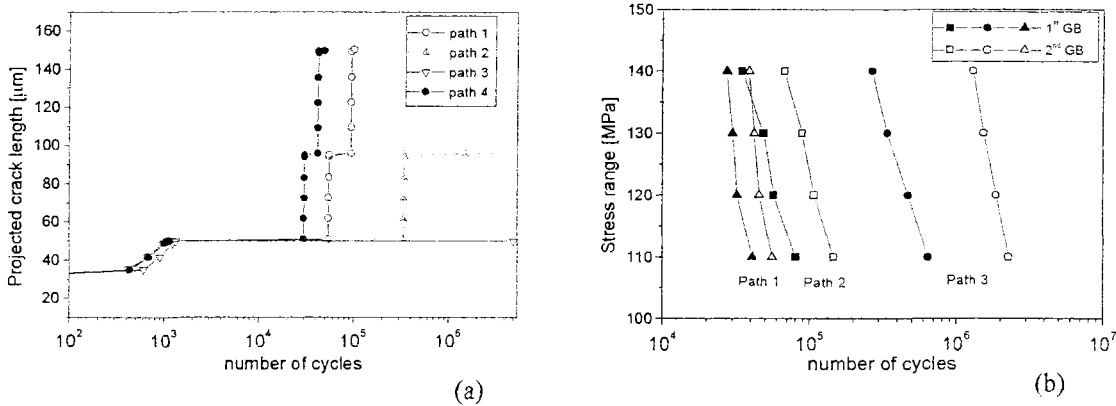


Figure 3: a- Evolution of the projected lengths for the different crack paths; b- Influence of the stress range.

The influence of the stress range is illustrated on figure 3-b that mimics a Wöhlers plot. The number of cycles needed to develop a crack, twice the mean grain size in length varies a lot with the crack path.

Figure 4 shows how the number of cycles needed for a crack to enter the second grain varies with the mean grain size. First it can be noticed that in accordance with experimental observations, most of the life is spent in arrest periods and very little in transgranular

propagation. Second, as the mean grain size increases, the stress concentration in the next grain gets higher, due to an increased SIF, and more space to pileup emitted dislocations, so that crack transfer becomes easier and the endurance is reduced, consistently with experimental results.

Many experimental data in the literature show that a few overload cycles may remove the endurance limit because these cycles enable arrested microcracks to cross microstructural obstacles. The present model reproduces this fact, as illustrated by figure 5. For a normal stress range of ± 110 MPa, forty five overload cycles at ± 140 MPa applied when the crack tip is close to the first and second GB reduce by a factor of two the number of cycles needed to grow the crack to the third grain.

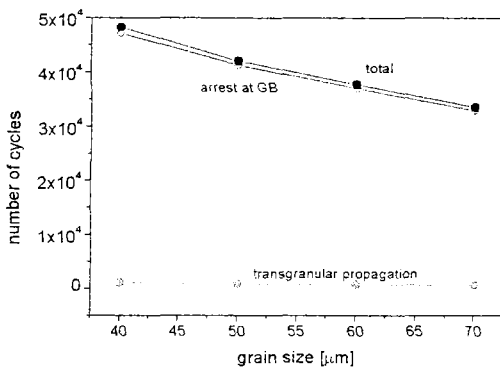


Figure 4: Variation of the number of cycles needed for a crack to enter the second grain with the mean grain size.

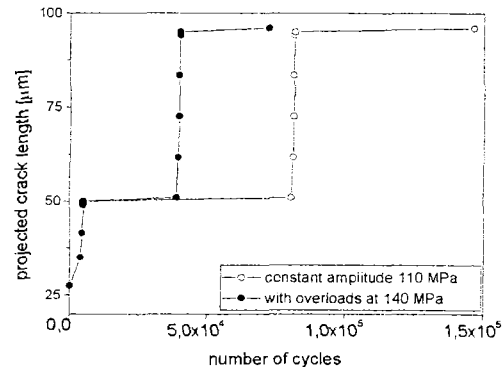


Figure 5: Influence of a few (45) overload cycles at ± 140 MPa on microcrack growth under ± 110 MPa.

CONCLUSIONS

Crystallographic propagation of fatigue cracks in a polycrystal under reversed torsion was modelled using local stresses computed by FE as input for discrete dislocation dynamics simulations. The simulations reproduce the scatter in microcracks growth rates associated with various local textures and an increased scatter for small loading ranges. Longer fatigue lives are predicted for small grain size materials. The decrease in the arrest periods at GBs as a crack develops is reproduced. The fact that overloads may suppress the endurance limit by unlocking microcracks arrested at GBs is also qualitatively described by the model.

REFERENCES

- [1] Doquet, V., *Fat. Fract. Eng. Mat. Struct.* **22**, pp 215-223, 1999.
- [2] Okazaki, M., *Met. Trans.*, **22A**, pp479-487, 1991.
- [3] Sun, Y., Beltz, G.E., Rice, J.R., *Mat. Sci. Eng.*, A170, pp 67-85, 1993.
- [4] Tanaka, K., Akinawa, Y., *Short fatigue cracks, mechanics and mechanisms*, pp 59-71, Ritchie, Ravichandran and Murakami eds, Elsevier 1998.
- [5] Head, A.K., *Phil. Mag.*, **44 n° 348**, pp 92-94, 1952
- [6] Zhai T., Wilkinson A., Martin J.W., *Acta Mater.*, **48**, pp 4917-27, 2000
- [7] Morris, W.L., James, M.R., Buck, O., *Met. Trans.* **12A**, pp 57-64, 1981

[8] Ludwig W., Buffière J.Y., Savelli S., Cloetens P., *Acta Materialia*, **51 N°3**, 2003.

Acknowledgements: The authors acknowledge the financial support of CEA, CNRS and EDF for the present study, carried out in the framework of the collaboration program SMIRN.